2023 IEEE International Conference on Systems, Man, and Cybernetics (SMC)
October 1-4, 2023, Oahu, Hawaii, USA

Add-if-Silent Rule-Based Growing Neural Gas with Amount of Movement for High-Density Topological Structure Generation of Dynamic Object

1st Masaya Shoji
ROBOTIS Co., Ltd.
Advanced Institute of Industrial Technology
Tokyo Metropolitan University
Tokyo, Japan
toukairinn@robotis.com

2nd Takenori Obo
Department of Mechanical Systems Engineering
Tokyo Metropolitan University
Tokyo, Japan
t.obo@tmu.ac.jp

3rd Naoyuki Kubota
Department of Mechanical Systems Engineering
Tokyo Metropolitan University
Tokyo, Japan
kubota@tmu.ac.jp

2023 IEEE International Conference on Systems, Man, and Cybernetics (SMC) | 979-8-3503-3702-0/23/$31.00 ©2023 IEEE | DOI: 10.1109/SMC53992.2023.10394107

***Abstract*— In order to realize a super-smart society (Society 5.0) where humans and robots coexist, there is a need for a perceptual system that can recognize the environment quickly and flexibly in an environment that changes from moment to moment. In an unknown environment, the characteristics of objects cannot be known in advance, and thus prior learning-based recognition methods such as deep reinforcement learning may not be able to cope with this situation. In this study, we construct a 3D topological map of the environment in real-time using Growing Neural Gas (GNG), which can learn 3D topological structures even for unlearned objects. However conventional GNG have the problem that they cannot generate nodes with high-density for distant objects and cannot identify whether an unknown object is static or dynamic. Therefore, by directly adding useful input data as a new node (reference vector) based on the object category labels of the winner nodes (nearest nodes) to the input vector (3D point cloud), it is possible to generate high-density topological structures even for distant objects. We proposed the Add-if-Silent rule-based GNG with Amount of Movement (AiS-GNG-AM), which can identify between static and dynamic objects based on the past amount of movement of a node. The effectiveness of the proposed method is verified through experiments using a 3D dynamics simulator.**

Keywords—Topological mapping, growing neural gas (GNG), high-density topological structure generation, perceptual system

I. INTRODUCTION

In recent years, in order to realize a super-smart society (Society 5.0) where humans and robots coexist, there is a need for a rapidly and flexible perceptual system that can recognize unknown objects in various unknown and dynamic environments. In particular, autonomous mobile robots and self-driving systems require a processing system that can process a huge amount of 3D point cloud data (distance information) acquired from 3D LiDAR and RGB-D cameras in real-time. A popular and widely used environment recognition method is the obstacle detector [1]. However, the recognition performance of this method is strongly dependent on the parameter settings, and can cause misrecognition, such as recognizing walls as small objects or failing to detect obstacles themselves, depending on the settings. Therefore, the parameters must be re-adjusted for each environment. Many environment recognition methods [2]-[4] have been proposed using RGB-D cameras that can combine distance and image information, but the performance of these methods is strongly dependent on the lighting conditions of the environment, resulting in unstable recognition results.

In this study, we construct a 3D topological map of the environment in real-time using Growing Neural Gas (GNG) [5], which can efficiently learn 3D topological structures for unlearned objects and can adapt to the environment in a self-organizing process without readjusting parameters. However, unsupervised learning methods such as conventional GNG [5] have a problem that they are not adaptive enough to learn appropriate topological structures when learning online in real environments, and a number of improvements have been proposed. Specifically, the conventional GNG method of deleting nodes based on the age of their edges was unable to correctly learn the 3D topological structure of the real environment because it was unable to quickly delete the nodes that were unnecessary. To improve adaptability in online learning, modified GNG with Utility (GNG-U2) [6] has been proposed, in which each node has a Utility value to evaluate its usefulness, and nodes with high accumulated error and low Utility values are directly removed. In addition, GNG-U2 can learn spatial and color information simultaneously by using weight vectors, which are called relative importance. However, its effectiveness in dynamic environments has not been verified.

Dynamic Density Growing Neural Gas (DD-GNG) [7] has been proposed, which prioritizes sampling from the area near unknown objects when detecting unknown objects and adjusts the Utility value according to the Strength value of the nodes to reduce the risk of deletion even when the nodes are densely generated and redundant nodes are many. DD-GNG can be used for vertical ladder detection [7], real-time grasping affordance detection for robot manipulation [8], and avoidance of sudden obstacles for multi-legged robots [9]. However, in the real world, because of the characteristics of RGB-D cameras, the sample density decreases for more far-away objects, and only sparse depth information can be obtained, the topological structure of unknown objects cannot be generated at high-density using any of the improved

Authorized licensed use limited to: Tokyo Metropolitan Industrial Tech Research Inst. Downloaded on May 28,2025 at 08:54:42 UTC from IEEE Xplore. Restrictions apply.

methods. In DD-GNG, the sampling process is performed focusing on unknown objects after detection, but when used as a perceptual system for mobile robots, etc., nodes must first be generated densely and detected as clusters in order to detect objects that are relatively far-away from the system. Also, conventional GNGs assigned object category labels, such as unknown objects, to each node based on the normal vector, but did not identify between static and dynamic objects. Considering its application to robots, it is important to identify between dynamic objects such as pedestrians and fixed obstacles for behavior control. Therefore, by directly adding useful input data as reference vectors based on the object category labels of the winner nodes (nearest nodes) to the input vector (point cloud), a high-density topological structure can be generated even for distant objects. We proposed Add-if-Silent rule-based GNG with Amount of Movement (AiS-GNG-AM), which can identify moving objects based on the past amount of movement of nodes. We verify the effectiveness of the proposed method through experiments using a 3D dynamics simulator.

This paper is organized as follows. Section II provides an overview of the proposed method. Section III describes the details of the proposed Add-if-Silent rule-based GNG with Amount of Movement (AiS-GNG-AM) and how it differs from the conventional method. In Section IV, the experimental results of the conventional and proposed methods are compared and discussed. Finally, in Section V, we conclude and discuss the effectiveness of the proposed model and future research directions.

II. System Overview

In this section, we describe an overview of the proposed method. Fig. 1 shows a flowchart of the proposed 3D topological map building system based on Add-if-Silent rule-based Growing Neural Gas with Amount of Movement (AiS-GNG-AM), which uses only 3D point cloud data. In the proposed method, a depth camera (RealSense D435) is used to acquire only 3D point cloud data. After down dumping using a voxel grid, the acquired data is input to the AiS-GNG-AM, which randomly samples predefined λ points ($\lambda = 300$) instead of using all points for learning. Once the GNG has generated a topological structure represented by nodes and edges, the nodes are assigned labels such as wall surface, floor surface (safe terrain), or unknown object based on the normal vectors calculated from the local triangulated surfaces. The calculations of the normal vectors and labeling are described in detail in our previous work [7]-[9].

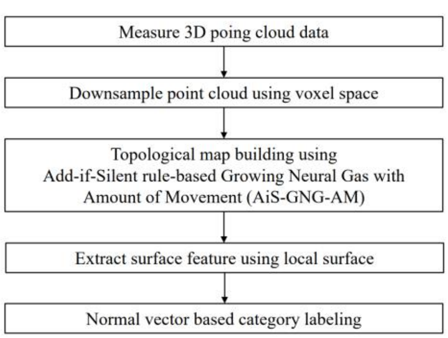

Fig. 1. Total flowchart of our proposed method

III. Add-if-Silent Rule-Based Growing Neural Gas with Amount of Movement

A. Growing Neural Gas with Amount of Movement

In GNG, the reference vector moves during learning, but it is not possible to identify whether each node is generated for a static or dynamic object by simply examining the amount of movement at each step. Therefore, as shown in Fig. 2, the proposed method uses the distance between the position of a node with the label of an unknown object at multiple steps in the past (4 steps in the example) and its position at the current time. The reference vector itself follows the object, moving in a certain direction and moving away from it. The amount of movement at multiple time step $\Delta dist(t)=h_i(t)-h_i(t-S)$ is fuzzified by the fuzzy membership function according to the following Eq. (1), and if it exceeds a predefined threshold value, the label of the reference node is assumed to be a dynamic object as shown in Eq. (2).

$$\mu_i^{Active}(\Delta dist_i(t)) = \begin{cases} \dfrac{|\Delta dist_i(t) - \alpha_{Active}|}{\beta_{Active}} & \text{if } |\Delta dist_i(t) - \alpha_{Active}| \le \beta_{Active} \\ 1 & \text{otherwise} \end{cases} \tag{1}$$

$$L_i = \{\text{Dynamic Object}\} \text{ if } \mu_i^{Active} \ge \theta_{Active} \tag{2}$$

where L_i is the object category label of the i-th reference node, $h_i(t)$ is the position of the reference vector with the unknown object label at discrete time t, S is the number of steps back in time, μ_i^{Active} is the degree of activity of the node (reference vector), $\Delta dist(t)$ is the distance traveled in multiple steps, α_{Active} and β_{Active} are the center value and width of the membership function, respectively, and θ_{Active} is the threshold value.

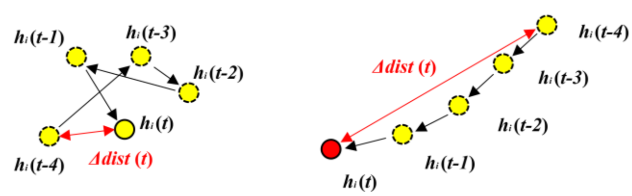

(a) Static Object (b) Dynamic object

Fig. 2. Concept of growing neural gas with amount of movement

B. Add-if-Silent Rule-Based Growing Process

In conventional GNG [5], [6], a node is added every time λ input vectors are learned from all input vectors (3D point cloud data) based on the accumulated error. However, in real-world environments, point clouds of object surfaces located far-away are rarely sampled, and even after repeated training, nodes are never generated densely enough to be detected as objects. In addition, DD-GNG [7]-[9] performs a focused sampling process after detecting unknown objects, but when used as a perceptual system for mobile robots, etc., in order to detect objects that are relatively far-away, it is necessary for nodes to be generated in high-density first, and then detected as clusters. However, due to the characteristics of RGB-D cameras, it is difficult to generate a high-density of nodes for objects that are far-away from the camera.

Authorized licensed use limited to: Tokyo Metropolitan Industrial Tech Research Inst. Downloaded on May 28,2025 at 08:54:42 UTC from IEEE Xplore. Restrictions apply.

Therefore, instead of adding nodes between reference vectors based on the accumulated error, this study proposes an AiS-GNG. At the stage of selecting the input vector, it is not yet known whether the input data exists on the surface of the unknown object. Then, if the first winner node and second winner node for the input vector have category labels corresponding to the unknown object, and both nodes exist within a predefined tolerance area, the input vector is added as a reference node without modification. If there is no neuron (node) that responds to the input that is useful for learning the 3D topological structure of an unknown object, a new neuron is added at that position, which is based on the Add-if -Silent rule [10]-[13], which is a learning rule used in the neo-cognition. The basic concept of AiS-GNG is shown in Fig. 3. As mentioned above, if the first and second winner nodes of an input vector lie within the allowed range and each has a label indicating either an unknown object category or a dynamic object category, then the input vector is judged useful for representing the unknown object surface and is added as a reference vector (Fig. 3(a), Fig. 3(b)). If the winner node is outside the allowed range (Fig. 3(c)) or if the label indicates other than unknown and dynamic objects (Fig. 3(d)), the reference vector is not added. This addition rule ensures that nodes are added directly when the input data are useful for learning unknown and dynamic objects and that no redundant nodes are added when a useful reference node already exists so that the phase structure is properly acquired.

The pseudo-code for the Add-if-Silent rule-based growing process is shown in Algorithm 1. Since much of the processing is common to GNG-U2 [9], a detailed description is omitted and only the processing specific to AiS-GNG-AM is described. In the first line of the algorithm, two conditions are checked: whether the labels L_i of the first and second winner nodes s_1 and s_2 are unknown objects or dynamic objects for the input vector, and whether the Euclidean distance from the input vector v_t to the winner nodes is within a tolerance area. If both conditions are satisfied, the node is considered to be useful input data and is added as a new node (reference vector). In this case, the reference vector h_r is the 3D position of input vector v_t, the accumulated error E_r and Utility value U_r of the newly created node r are the average value of s_1 and s_2, and the label L_r is an unknown object. The Strength value δ_r is set to 1000 and the deletion condition is $E_u/U_l > k*\delta_r$ as in DD-GNG [7] to make it difficult to delete. Each node is labeled according to its normal vector, but may also be labeled as a moving object based on the amount of movement described above. This Algorithm 1 is executed at the same time as the search for the winner node, and if the condition is not satisfied, it does not add any nodes. In addition, when the label of the added node (reference vector) is replaced with a safe terrain, the strength value δ_r is reset to 1.0 to make it easily deletable.

Algorithm 1 Add-if-Silent Rule-Based Growing Process

1: **if** $L_{s1}=L_{s2}=$ {Unknown Object or Dynamic Object} and $\theta^{AiS}_{Min} < \|v_t - h_{s1}\| < \theta^{AiS}_{Max}$ and $\theta^{AiS}_{Min} < \|v_t - h_{s2}\| < \theta^{AiS}_{Max}$ **then**

2: $h_r = v_t$, $E_r = 0.5\cdot(E_{s1}+E_{s2})$, $U_r = 0.5\cdot(U_{s1}+U_{s2})$, $\delta_r = 1000$, $L_r = \{\text{Unknown Object}\}$

3: $A \leftarrow A + \{r\}$

4: $c_{r,s1} = 1,\quad c_{r,s2} = 1$

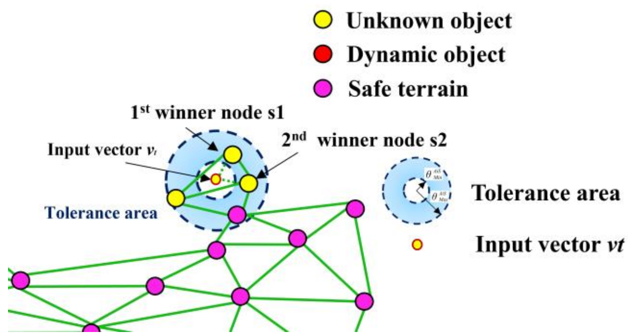

(a) Case1

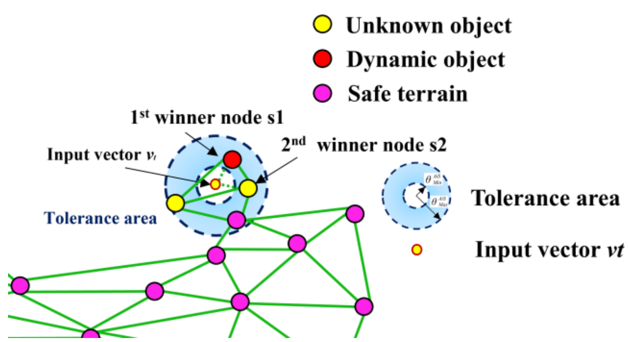

(b) Case2

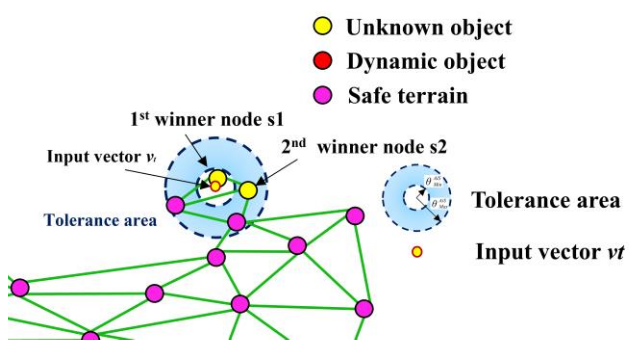

(c) Case3

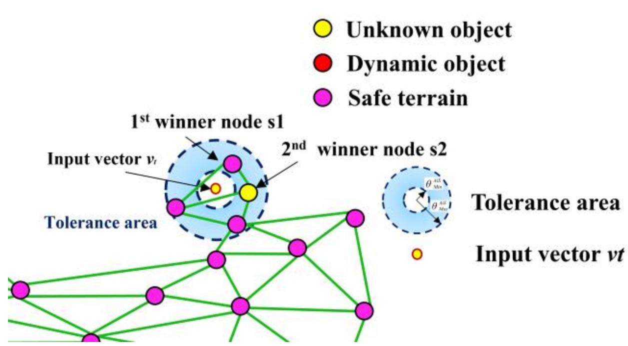

(d) Case4

Fig. 3. Add-if-Silent rule-based growing process

Authorized licensed use limited to: Tokyo Metropolitan Industrial Tech Research Inst. Downloaded on May 28,2025 at 08:54:42 UTC from IEEE Xplore. Restrictions apply.

IV. EXPERIMENTAL RESULT

A. Experimental Conditions

Gazebo [14], an open-source 3D dynamics simulator, was used as the physical simulation environment. The mobile robot used in the experiments is shown in Fig. 4. TurtleBot3 is an official ROS platform [15] that can be easily customized for different purposes. In this study, we use TurtleBot3 Big Wheel 3RS [16] equipped with three RGB-D cameras (Intel RealSense D435i). This robot can handle point cloud data on the simulator as well as on the real robot.

In this experiment, only depth information was used, and the measurement range was set to 0.2 [m]-10.0 [m], the same as the actual RealSense D435 specifications. The resolution can be the same as that of the actual device, and in this case, the coarsest resolution of 424×240 [pixels] was used to reduce the computation cost, and the sampling rate (frame rate) was set to 30 [fps]. Since there are three RGB-D cameras mounted on the robot, the horizontal field of view is 212.5 [deg]. The robot does not move, since the objective of this experiment is to generate high-density topological structures for far-away objects and moving object (pedestrian).

The experimental environments are then shown in Figs. 5 to 7. Case 1 is intended to analyze whether or not unknown objects are misdetected for nodes generated in an environment with three static objects (Fig. 5); Case 2 is intended to analyze how many nodes with dynamic object labels are generated in an environment with only pedestrians (Fig. 6). Here, the pedestrian travels from a point 8.0 [m] directly in front of the robot to a point 2.0 [m] in front of the robot, a total of 6.0 [m], at a travel speed of 1.0 [m/s] and back. The last case, Case 3, aims to analyze how nodes are generated in a mixed environment of static and dynamic objects with three static objects and one pedestrian who moves as in Case 2.

The computer used in the experiment was an Intel NUC Core i7 with 8GB of RAM without any GPU installed, and all GNG common parameter settings are the same as in the previous study [6]. In addition, the unique parameter of AiS-GNG-AM, $\theta^{AiS}_{Min} = 0.25$, $\theta^{AiS}_{Max} = 0.50$, $\alpha_{Active} = 0.0$, $\beta_{Active} = 0.1$, $\theta_{Active} = 0.9$, $S = 4$. Also, the conventional method GNG-U2 can also learn spatial (3D space) and color information at the same time, but in order to conduct a comparison experiment under the same conditions as AiS-GNG-AM, only the spatial information (3D point cloud data) was used as input to generate topological structures.

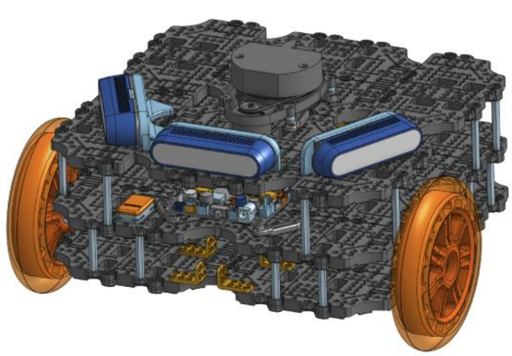

Fig. 4. TurtleBot3 Big Wheel 3RS (ROBOTIS Japan Custom) [16]

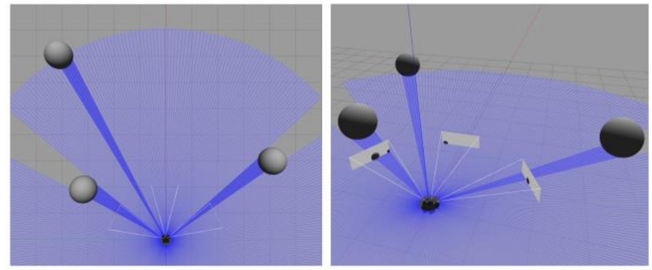

(a) Top view (b) Overhead view

Fig. 5. Experimental environment-Case1

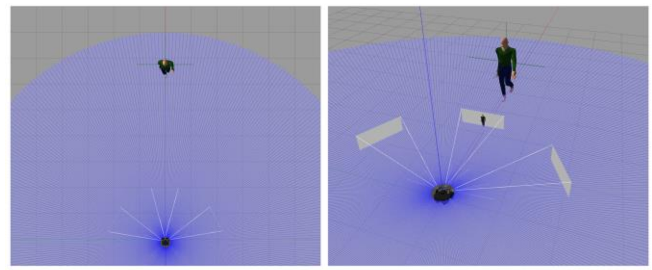

(a) Top view (b) Overhead view

Fig. 6. Experimental environment-Case2

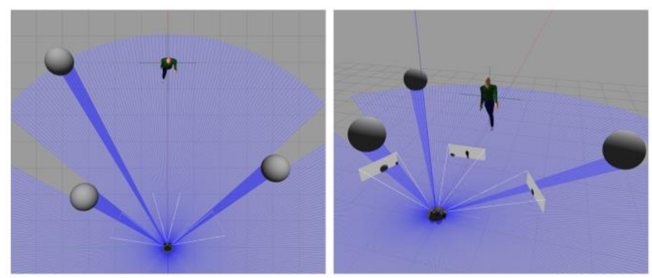

(a) Top view (b) Overhead view

Fig. 7. Experimental environment-Case3

B. Experimental Results

Fig. 8, Fig. 9, and Fig. 10 show the experimental results comparing the application of the conventional method GNG-U2 [6] and the AiS-GNG-AM proposed in this paper in the same environment (Case 1 to Case 3). The small yellow sphere represents a GNG reference node labeled as an unknown object, the small red sphere represents a GNG reference node labeled as a dynamic object, and the small pink sphere represents a GNG reference node labeled as a safe area (floor).

The conventional method shown in Fig. 8(a) produced a few nodes labeled as unknown objects for both near and far objects, and a large proportion of nodes were labeled as dynamic objects relative to static objects. This is thought to be due to the inability to generate nodes with high-density for unknown objects, resulting in a large movement of the few nodes, which were mis-detected as dynamic objects. The proposed method generates very high-density nodes for all static objects, both near and far, indicating that it can adequately learn the topological structure of unknown objects and that the percentage of nodes with dynamic object labels is also quite low (Fig. 8(b)).

Authorized licensed use limited to: Tokyo Metropolitan Industrial Tech Research Inst. Downloaded on May 28,2025 at 08:54:42 UTC from IEEE Xplore. Restrictions apply.

Next, let us look at Case 2, where there is only one pedestrian moving at 1.0 [m/s]. We can see that the conventional method generates nodes with labels of unknown objects and dynamic object, both of which are extremely small in number and cannot represent the shape of the dynamic object (pedestrian) (Fig. 9(a)). The proposed method is able to generate a high-density of nodes even for moving objects, and the unknown object labels are reattached to dynamic object labels based on the amount of movement, and the topological structure can be correctly learned by nodes with many moving object labels (Fig. 9(b)). Finally, looking at the results for Case 3, which has three static unknown objects and one pedestrian moving at 1.0 [m/s], we see that the conventional method generates few nodes for all objects and fails to learn the shape of either static or dynamic objects (Fig. 10(a)). On the other hand, the proposed method generates a high-density of nodes with unknown object (static) labels for the three static objects and a high-density of nodes with dynamic object labels for the pedestrian (Fig. 10(b)). This indicates that the proposed Add-if-Silent rule can clearly identify dynamic and static objects, because nodes generated densely have a higher Strength value and are less likely to be deleted, and thus retain a history of the amount of movement. This indicates that the system is able to clearly identify between dynamic and static objects. However, it is also observed that a small number of nodes with dynamic object labels are generated for static objects as well. This may be due to the fact that the boundary region between a static object and the floor surface is more prone to node movement during training, and thus more likely to be falsely detected as a dynamic object, and further study is needed.

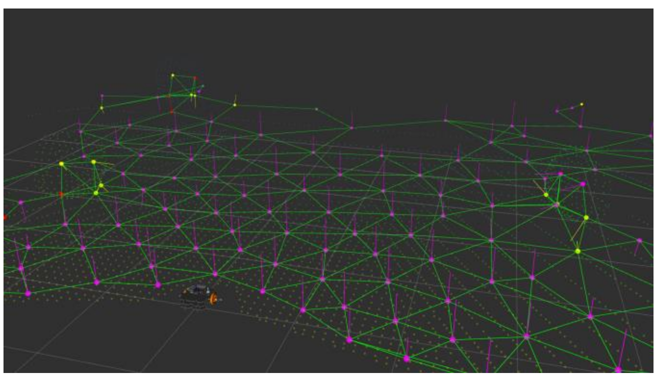

(a) Conventional method (GNG-U2)

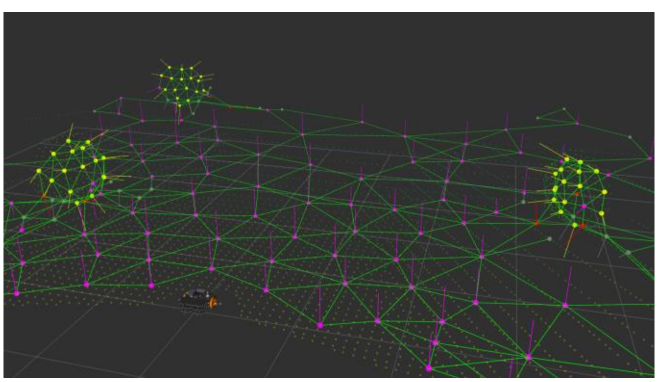

(b) Proposed method (AiS-GNG-AM)

Fig. 8. Topological structure generation in Case1

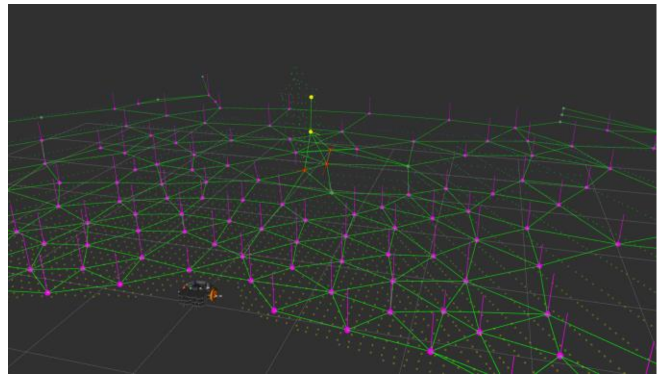

(a) Conventional method (GNG-U2)

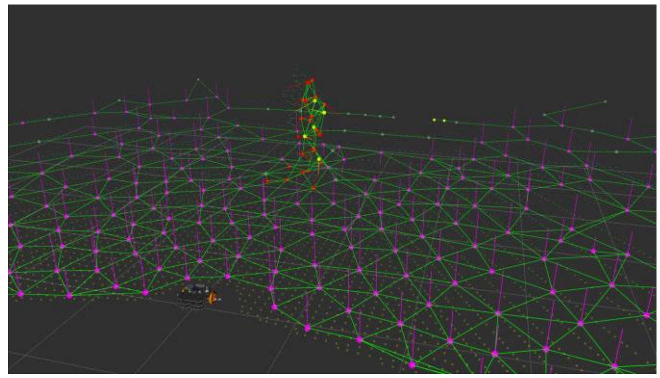

(b) Proposed method (AiS-GNG-AM)

Fig. 9. Topological structure generation in Case2

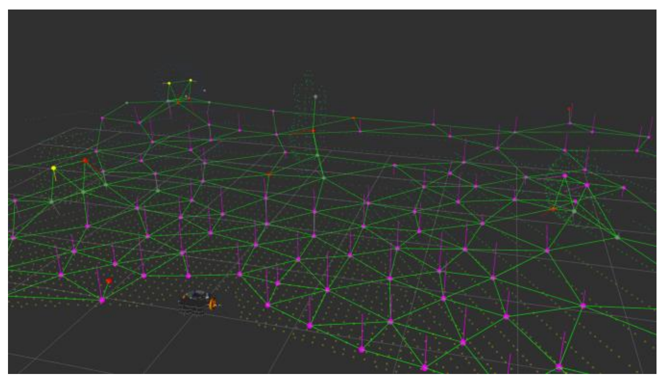

(a) Conventional method (GNG-U2)

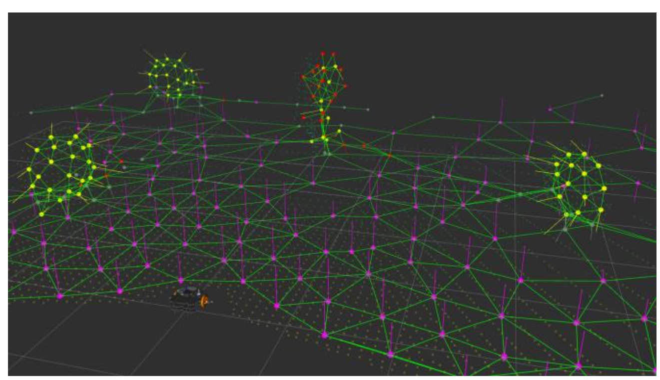

(b) Proposed method (AiS-GNG-AM)

Fig. 10. Topological structure generation in Case3

Authorized licensed use limited to: Tokyo Metropolitan Industrial Tech Research Inst. Downloaded on May 28,2025 at 08:54:42 UTC from IEEE Xplore. Restrictions apply.

Next, Fig. 11 to Fig. 13 show the transition of the total number of nodes in the GNG, the transition of the number of nodes with unknown object labels, and the transition of the number of nodes with dynamic object labels in each environment. In Case 1, the total number of nodes for the conventional method is about 150, indicating that the number of nodes for the proposed method is always about 50 larger (Fig. 11(a)). And the number of nodes with labels of unknown and dynamic objects is larger in the proposed method than in the conventional method by that number (Fig. 12(a), Fig. 13(a)). In Case 1, we can say that it is a misclassification because there are no dynamic objects, but in fact they are generated in a distributed manner. So, in reality, the objects are generated in a distributed manner, they are not generated at high-density, and there seems to be no problem in discriminating between static and dynamic objects. Next, in Case 2, we can see that the total number of nodes is about 300 for the proposed method while the conventional method has about 150 (Fig. 11(b)). In addition, the number of nodes with labels of unknown objects is almost none for the conventional method and about 15 for the proposed method, indicating that the labels of unknown objects generated for pedestrians are immediately changed to labels for dynamic objects (Fig. 12(b)). Therefore, there is a very large difference in the number of nodes with dynamic object labels, indicating that the proposed method generates significantly more nodes (Fig. 13(b)). Compared to Case 1, the number of nodes with dynamic object labels is significantly higher in Case 2, indicating that the proposed method can appropriately identify moving objects such as pedestrians based on the amount of node movement. Next, in Case 3, as in Case 2, the total number of nodes is about 150 for the conventional method, while the number is about 300 for the proposed method (Fig. 11(c)). The number of nodes with labels of unknown objects is about 20 for the conventional method, while the number is about 80 for the proposed method, indicating that the proposed method is able to generate nodes with high-density for pedestrians (Fig. 12(c)). This is a correct behavior because the number of static objects has increased. There is also a significant difference in the number of nodes with dynamic object labels, indicating that the proposed method generates significantly more nodes (Fig. 13(c)). In Case 3, the proposed method was able to identify static unknown objects and moving objects such as pedestrians, and generate a high-density of nodes with appropriate labels for each.

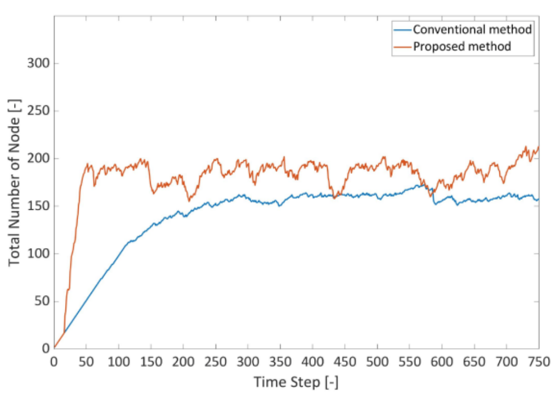

(a) Case1

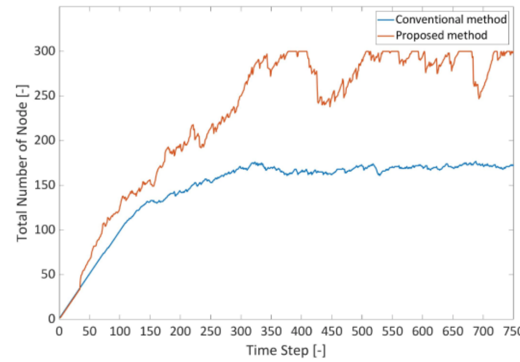

(b) Case2

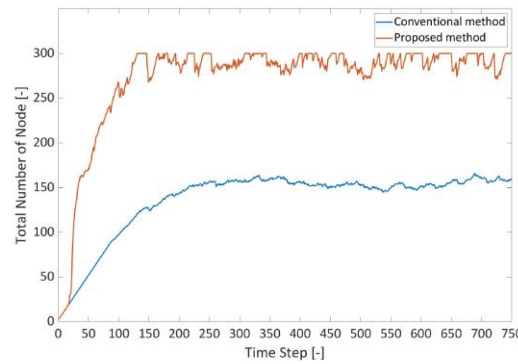

(c) Case3

Fig. 11. The transition of the total number of nodes

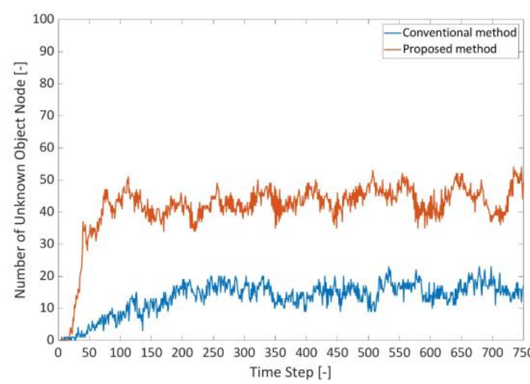

(a) Case1

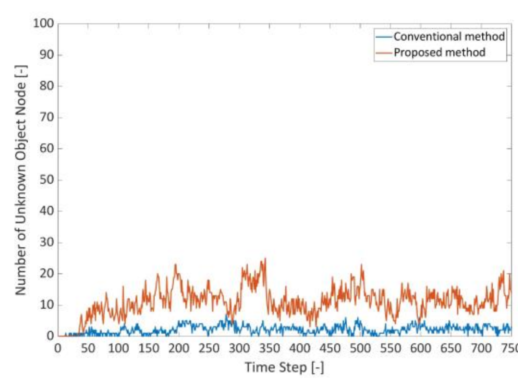

(b) Case2

Authorized licensed use limited to: Tokyo Metropolitan Industrial Tech Research Inst. Downloaded on May 28,2025 at 08:54:42 UTC from IEEE Xplore. Restrictions apply.

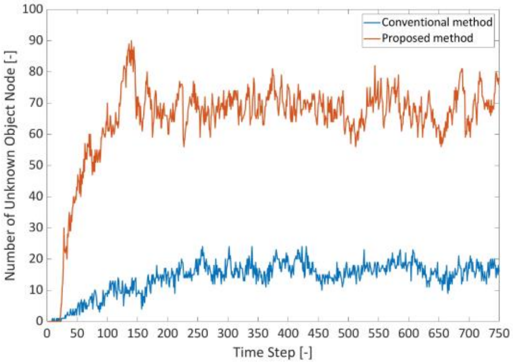

(c) Case3

Fig. 12. The transition of the number of unknown object nodes

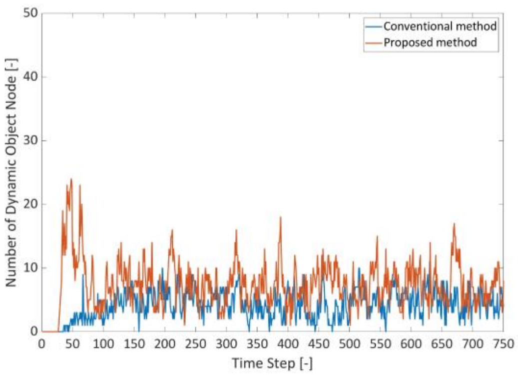

(a) Case1

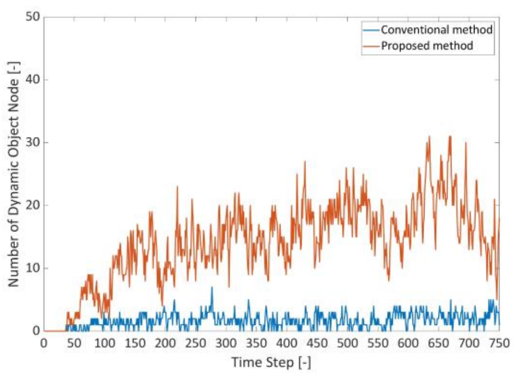

(b) Case2

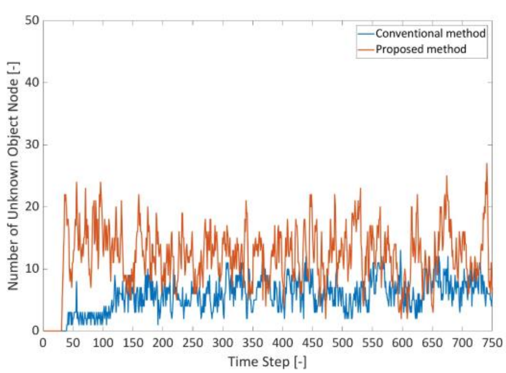

(c) Case3

Fig. 13. The transition of the number of dynamic object nodes

Finally, the processing time results are shown in Fig. 14: in Case 1, the difference between the conventional and proposed methods is not so large (Fig. 14(a)), while in Cases 2 and 3, the difference in processing time increases with the number of nodes generated for unknown and dynamic objects (Fig. 14(b), (c)). This is because the difference in the total number of nodes increases as the number of unknown objects increases, and due to the characteristics of GNG, the computational cost of the Euclidean distance between the input vector (3D point cloud data) and the reference vector increases as the number of nodes increases. However, the proposed method, including Case 1 to Case 3, is within about 50 [msec], which is well within the practical range for operation in a real system.

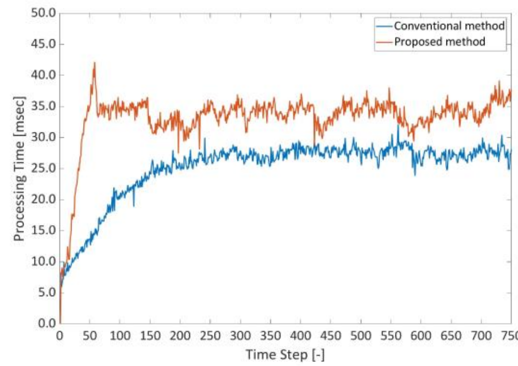

(a) Case1

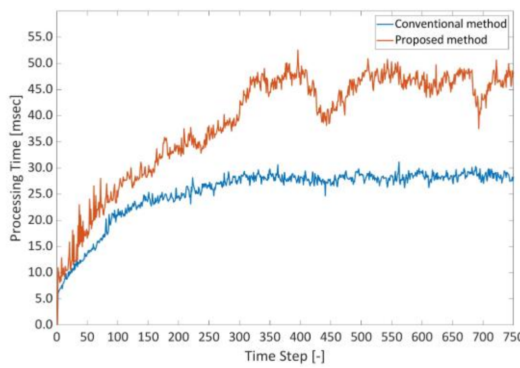

(b) Case2

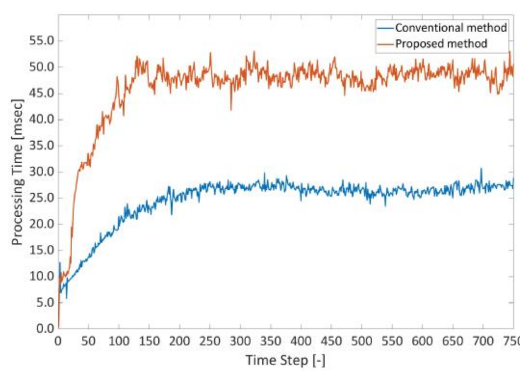

(c) Case3

Fig. 14. The transition of the processing time

Authorized licensed use limited to: Tokyo Metropolitan Industrial Tech Research Inst. Downloaded on May 28,2025 at 08:54:42 UTC from IEEE Xplore. Restrictions apply.

V. CONCLUSION

In this study, we solved the problem that conventional GNG cannot generate high-density topological structures of unknown objects in a 3D spatial environment due to the characteristics of RGB-D cameras, where the sample density decreases for more distant objects, and cannot identify between static and dynamic objects. We proposed an Add-if-Silent rule-based Growing Neural Gas with Amount of Movement (AiS-GNG-AM). Experiments using a 3D dynamics simulator confirmed that the proposed method can generate densely labeled nodes for multiple distant unknown objects and can learn 3D topological structures appropriately even for moving objects such as pedestrians. It was also shown that the number of labeled nodes increases as the number of objects increases to represent the geometry of unknown and dynamic objects and that the processing time increases only a reasonable amount of computation for each additional node, indicating that the learning is fast.

In the future, we would like to detect clusters using nodes with moving object labels and work on applications such as obstacle avoidance problems for mobile robots in dynamic environments and cognitive map building based on long-term memories of nodes.

ACKNOWLEDGMENT

This work was partially supported by JST [Moonshot R\&D][Grant Number JPMJMS2034].

References

[1] M. Przybyła, "Detection and tracking of 2D geometric obstacles from LRF data," 2017 11th International Workshop on Robot Motion and Control (RoMoCo), Wasowo Palace, Poland, 2017, pp. 135-141, doi: 10.1109/RoMoCo.2017.8003904.

[2] Andrew Wing Keung, Gay Paul and Dikai Liu, "Surface-type classification using RGB-D", Automation Science and Engineering IEEE Transactions on 11.2, pp. 359-366, 2014.

[3] Julia Diebold et al., "Interactive multi-label segmentation of RGB-D images." in Scale Space and Variational Methods in Computer Vision, Springer International Publishing, pp. 294-306, 2015.

[4] J. Strom, A. Richardson and E. Olson, "Graph based segmentation of colored 3d laser point clouds", Proc. of the IEEE/RSJ International Conference on Intelligent Robots and Systems (IROS), 2010.

[5] B. Fritzke, "A growing neural gas network learns topologies", Advances in Neural Information Processing Systems, vol. 7, pp. 625-632, 1995.

[6] Y. Toda, Zhaojie Ju, Hui Yu, N. Takesue, K. Wada and N. Kubota, "Real-time 3D point cloud segmentation using Growing Neural Gas with Utility," 2016 9th International Conference on Human System Interactions (HSI), Portsmouth, UK, 2016, pp. 418-422, doi: 10.1109/HSI.2016.7529667.

[7] A. A. Saputra, W. H. Chin, Y. Toda, N. Takesue and N. Kubota, "Dynamic Density Topological Structure Generation for Real-Time Ladder Affordance Detection," 2019 IEEE/RSJ International Conference on Intelligent Robots and Systems (IROS), Macau, China, 2019, pp. 3439-3444, doi: 10.1109/IROS40897.2019.8968003.

[8] A. A. Saputra, C. W. Hong and N. Kubota, "Real-time Grasp Affordance Detection of Unknown Object for Robot-Human Interaction," 2019 IEEE International Conference on Systems, Man and Cybernetics (SMC), Bari, Italy, 2019, pp. 3093-3098, doi: 10.1109/SMC.2019.8914202.

[9] A. A. Saputra, J. Botzheim, A. J. Ijspeert and N. Kubota, "Combining Reflexes and External Sensory Information in a Neuromusculoskeletal Model to Control a Quadruped Robot," in IEEE Transactions on Cybernetics, vol. 52, no. 8, pp. 7981-7994, Aug. 2022, doi: 10.1109/TCYB.2021.3052253.

[10] Fukushima, Kunihiko. "Add-if-Silent Rule for Training Multi-layered Convolutional Network Neocognitron." International Conference on Neural Information Processing (2014).

[11] Fukushima, K.: Artificial Vision by Multi-layered Neural Networks: Neocognitron and its Advances. Neural Networks 37, 103–119 (2013).

[12] Fukushima, K.: Training Multi-layered Neural Network Neocognitron. Neural Networks 40, 18–31 (2013).

[13] Fukushima, K.: One-shot Learning with Feedback for Multi-layered Convolutional Network. In: Wermter, S., Weber, C., Duch, W., Honkela, T., Koprinkova-Hristova, P., Magg, S., Palm, G., Villa, A.E.P. (eds.) ICANN 2014. LNCS, vol. 8681, pp. 291–298. Springer, Heidelberg (2014)

[14] https://gazebosim.org/home

[15] ROBOTIS Co., Ltd. , "e-Manual TurtleBot3", https://emanual.robotis.com/docs/en/platform/turtlebot3/overview/

[16] ROBOTIS Co., Ltd. , "TurtleBot3 Friends: Big Wheel 3RS", https://github.com/ROBOTIS-JAPAN-GIT/turtlebot3_jp_custom/blob/master/README_en.md

Authorized licensed use limited to: Tokyo Metropolitan Industrial Tech Research Inst. Downloaded on May 28,2025 at 08:54:42 UTC from IEEE Xplore. Restrictions apply.